Mon. Not. R. Astron. Soc. **000**, 000–000 (0000) Printed 4 October 1999 (MN LaTeX style file v1.4)

High precision magnetic field measurements of Ap and Bp stars*

G.A. Wade[1], J.-F. Donati[2], J.D. Landstreet[2,3], S.L.S. Shorlin[3]
[1] *Astronomy Department, University of Toronto at Mississauga, Mississauga, Ontario, Canada L5L 1C6*
[2] *Observatoire Midi-Pyrénées, 14 Avenue Edouard Belin, 31400 Toulouse, France*
[3] *Physics & Astronomy Department, The University of Western Ontario, London, Ontario, Canada, N6A 3K7*

4 October 1999

ABSTRACT

In this paper we describe a new approach for measuring the mean longitudinal magnetic field and net linear polarisation of Ap and Bp stars. As was demonstrated by Wade et al. (1999a), Least-Squares Deconvolution (LSD; Donati et al. 1997) provides a powerful technique for detecting weak Stokes V, Q and U Zeeman signatures in stellar spectral lines. These signatures have the potential to apply strong new constraints to models of stellar magnetic field structure. Here we point out two important uses of LSD Stokes profiles. First, they can provide very precise determinations of the mean longitudinal magnetic field. In particular, this method allows one to frequently obtain 1σ error bars better than 50 G, and smaller than 20 G in some cases. This method is applicable to both broad and sharp lined stars, with both weak and strong magnetic fields, and effectively redefines the quality standard of longitudinal field determinations. Secondly, LSD profiles can in some cases provide a measure of the net linear polarisation, a quantity analogous to the broadband linear polarisation recently used to derive detailed magnetic field models for a few stars (e.g. Leroy et al. 1996). In this paper we report new high precision measurements of the longitudinal fields of 14 magnetic Ap/Bp stars, as well as net linear polarisation measurements for 4 of these stars, derived from LSD profiles.

Key words: stars: chemically peculiar – stars: magnetic fields – polarisation

1 INTRODUCTION

Some chemically peculiar Ap and Bp stars display magnetic fields which are directly detectable by means of the Zeeman effect in their spectral lines. The canonical diagnostic of these fields is the mean longitudinal magnetic field (or longitudinal field), the line-of-sight component of the field suitably weighted and integrated over the visible stellar disc, a quantity determined from measurements of Zeeman spectral line circular polarisation. Essentially all models of the geometry and detailed structure of the magnetic fields of these stars have been constrained using longitudinal field measurements, underscoring the important rôle of these data in understanding magnetism in upper-main sequence stars. In addition, longitudinal field measurements provide a fundamental method for determining the rotational periods of magnetic stars.

Longitudinal field measurements furthermore represent the standard method for searching for magnetic fields in further categories of stars. Searches for magnetic fields in other types of chemically peculiar stars (e.g. Landstreet 1982; Borra & Landstreet 1980; Borra, Landstreet & Thompson 1983; Bohlender & Landstreet 1990a), in pre-main sequence A and B type stars (Glagolevski & Choutonov 1998), in evolved A and B type stars (Elkin 1998), and in normal F through O type stars (Landstreet 1982) have relied almost exclusively on the longitudinal field as a quantitative magnetic field diagnostic.

The typical 1σ uncertainties associated with modern longitudinal field measurements (i.e. those acquired using electronic detectors) are around 200-300 G (Borra & Landstreet 1980; Mathys 1991; Mathys & Hubrig 1997; Wade et al. 1996, 1997). They are seldom better than 100 G, and are often worse than 300 G for broad-lined or faint stars (e.g. Borra & Landstreet 1980; Mathys 1991; Mathys & Hubrig 1997).

Two methods of field measurement have been responsible for the vast majority of modern measurements: the Balmer-line Zeeman analyser technique (e.g. Landstreet

* Based on observations obtained using the MuSiCoS spectropolarimeter at the Pic du Midi observatory, France

1982) and metallic-line spectropolarimetry (sometime referred to as the "photographic technique"). The precision of measurements of A and B stars obtained using the Balmer-line Zeeman analyser is determined primarily by photon flux, and is nearly independent of $v \sin i$. Because the method uses the polarisation information content of only a single, broad (Balmer) spectral line, this method requires a relatively long integration time to achieve a level of S/N similar to that which can be obtained from many metal lines in a sharp-line star, but it is competitive for broad-line stars. The best measurements obtained using this technique are thus for very bright stars. Example of such data are field measurements of the magnetic Ap stars ϵ UMa (Bohlender & Landstreet 1990b) and θ Aur (Borra & Landstreet 1980), for which best uncertainties of respectively 35 and 40 G were achieved. Landstreet (1982) also reported measurements of some 11 bright, apparently non-magnetic stars for which typical uncertainties of the order of 60 G were obtained. All the stars for which measurements of this accuracy have been obtained are brighter than V magnitude 4. This last paper also discusses in detail the S/N ratios achievable by various techniques.

The precision of measurements obtained from metal line spectropolarimetery, on the other hand, is determined by photon flux, line sharpness, and the number of lines observed. The principal weakness of this method is that it is quite sensitive to $v \sin i$; precision falls off rapidly with increasing line width. The best measurements obtained using this technique are therefore for bright stars with narrow lines. Early precision field measurements using a single strong line of Fe II were reported by Landstreet (1982), who reached an uncertainty of 7 G for Procyon. Errors of less than 50 G were achieved for about 10 other stars brighter than V magnitude 4.5. The precision of such measurements can be substantially improved by the simultaneous measurement of a number of spectral lines. Mathys & Hubrig (1997) were able to report uncertainties as small as 45 and 55 G respectively for β CrB ($V = 3.6$) and γ Equ ($V = 4.7$), both of which have $v \sin i \lesssim 3$ km s^{-1}.

From this discussion one should carry away two important facts. First, each of these commonly employed methods has its own suite of strengths and limitations, its own regime in which it is competitive. Secondly, while they are capable of obtaining very high precisions, this is possible only in exceptional circumstances which must be tailored to the specific method. The uncertainties which are obtained *typically*, as discussed above, for the brighter common magnetic Ap stars (with $m_V = 5 - 6$) are around 200-300 G, and are seldom better than 100 G. Given that magnetic fields with corresponding longitudinal fields weaker than 100 G are capable of having substantial effects on stellar atmospheres and envelopes (see for example Bohlender & Landstreet 1990b; Donati & Wade 1999) and that about half of magnetic Ap stars have rms longitudinal fields weaker than $\sim$ 300 G (Bohlender & Landstreet 1990a), the ability to commonly achieve precisions significantly better than 100 G would be a very useful step forward.

While the longitudinal field remains the canonical diagnostic of magnetic fields in stars, other kinds of data can be obtained which can constrain further the geometry and structure of the surface magnetic field. Some A and B type stars with strong fields and rich, strong line spectra exhibit a weak net linear polarisation (relative polarisation levels of a few times 10^{-4}, with uncertainties typically 1.0×10^{-4}) when observed photopolarimetrically in broad spectral bands (e.g. Kemp & Wolstencroft 1974; Leroy 1995a). This polarisation is thought to result from the differential saturation of the σ and π Zeeman components in strong lines (Leroy 1962, Calamai et al. 1975), and provides a strong constraint on the transverse component of the magnetic field. It has recently allowed investigators to construct the most detailed models of the magnetic field structure of A and B type stars (Leroy 1995a; Wade et al. 1996; Leroy et al. 1996). Net broadband linear polarisation can however only be obtained for those stars for which interstellar polarisation is rather small ($\lesssim 10^{-3}$ in relative units), and is not detected for many stars with sparse line spectra or with more complex field topologies. In addition, while the degree of accuracy and reproducibility of the longitudinal field has been tested by many investigators using a number of different methods, essentially all net linear polarisation measurements have been obtained photopolarimetrically; i.e. they are from a single kind of broadband measurement. As will become clear later in this paper, net linear polarisation measurements from LSD profiles *require* that the polarisation be generated within spectral lines (as opposed to the continuum). Therefore such measurements should allow us to confirm what has previously only been supposed: the broadband linear polarisation measured with photoelectric polarimeters *is* due to saturated linear polarisation within the lines. Both the extension of our ability to acquire net linear polarisation measurements (by allowing measurement of stars inaccessible via the current technique) and an opportunity to test the accuracy, reproducibility and theoretical understanding of broadband measurements would represent important contributions.

2 LEAST-SQUARES DECONVOLUTION

Least-Squares Deconvolution is cross-correlation technique developed specifically for the detection and measurement of weak polarisation signatures in stellar spectral lines. The method is described in detail by Donati et al. (1997) and Wade et al. (1999a; hereinafter WDLS) and is applied to Stokes V, Q and U spectra obtained using the MuSiCoS spectropolarimeter (Donati et al. 1999) by WDLS. At each observed phase and for each observed Stokes parameter Wade et al. report an LSD profile. These profiles are of very high signal-to-noise ratio (S/N), with relative noise levels around 10^{-4}. Stokes V signatures are typically detected at better than the 100σ level, while typically Stokes Q and U signatures are more modestly detected at around the 5-50σ level. In our analysis here we employ the same profiles presented by WDLS, extracted using the LSD line masks which they describe. We have not employed masks tailored to individual stars' abundances, nor have we restricted the spectral range of the deconvolution to obtain a better match with previously published data from smaller spectral windows (the spectral range employed is approximately 450-660 nm).

LSD is in many ways similar to other multi-line techniques such as the Moment Technique (a metallic-line method; Mathys 1989), in that it attempts to sum the signal in many spectral lines to increase the effective S/N. LSD is capable of achieving much better precision because it takes advantage of the signal contained in effectively all strong lines in the stellar spectrum, whereas the Moment Technique is only capable of using effectively unblended lines. LSD furthermore offers the advantage that it produces a mean Stokes V profile, deconvolved from the stellar spectrum. Because magnetic fields with complex topologies (see for example Donati et al. 1997) can produce weak Stokes V signatures which are consistent with zero longitudinal field, LSD can allow us to unambiguously detect such complex fields even in the case where the longitudinal field is null and the Stokes V profiles rather complex. While this is in principle possible using the Moment Technique, the low order moments which have been measured (up to second order for Stokes V) are probably not sufficient for such a task.

As is discussed by WDLS, LSD propagates photon statistical uncertainties (when available) from the reduced polarisation spectra, and thereby assigns a standard error bar to every spectral pixel in the LSD profile. These error bars can be used to assign theoretical uncertainties to longitudinal field and net linear polarisation measurements obtained from LSD profiles. However, because of the schematic modeling of the spectrum employed by LSD (described in more detail by WDLS) the realised uncertainties in LSD profiles tend to be larger than the estimate derived from pure photon noise statistics when the polarisation signatures detected in individual line profiles largely exceed in amplitude the local photon noise (i.e. when the convolution description of the model spectrum gets very poor). This underrepresentation of the real noise level by the photon statistical error bars is compensated for by scaling the photon noise statistical error bars of LSD profiles by a factor equal to the square root of the reduced χ^2 of the spectrum of $O-C$ residuals whenever this value exceeds unity. In Ap stars such scaling is almost always required for Stokes V ($O-C$ reduced $\chi^2 \gg 1$), while for Stokes Q and U (which have profiles in individual spectral lines almost always smaller than the local photon noise) the photon noise description is adequate ($O-C$ reduced $\chi^2 \simeq 1$).

Finally, the observing procedure employed by WDLS to obtain the spectropolarimetric measurements used in this paper also produces a diagnostic null, or N, spectrum associated with each stellar V, Q or U spectrum. LSD profiles extracted from the N spectra provide a high-precision, photon-limited evaluation of any spurious contribution to the profile. LSD profiles extracted from N spectra are used to show that no spurious contributions to the longitudinal field or net linear polarisaton variations are detected.

In the following sections we describe the manner in which longitudinal field and net linear polarisation measurements are obtained from LSD profiles. We then report measurements of the longitudinal field and net linear polarisation for individual stars and discuss the accuracy and precision of the measurements and in particular discuss whether or not the theoretical error bars associated with these measurements are consistent with the empirical uncertainties. We conclude with a summary of these results and some suggestions for useful applications of this approach.

2.1 Longitudinal magnetic field measurements

The mean longitudinal magnetic field (B_ℓ) is the line-of-sight component of the stellar magnetic field, suitably weighted and integrated over the visible stellar disk. It can be expressed as the first-order moment of the Stokes V Zeeman profile (Mathys 1989; Donati et al. 1997):

$$B_\ell = -2.14 \times 10^{11} \frac{\int vV(v)\, dv}{\lambda z c \int [I_c - I(v)]\, dv}, \tag{1}$$

where the wavelength λ is in nm and B_ℓ is in gauss. The Landé factor z is a mean value obtained from all lines used to compute the LSD profile. Although Eq. (1) is derived for analysis of a single spectral line, we use it here to interpret LSD measurements. This assumes that LSD profiles behave in many respects like individual spectral lines, an hypothesis that will be verified *a posteriori*.

Integration limits for B_ℓ measurements have been chosen by visually determining the extent of the line from the LSD Stokes I profile. The limits are asymmetric due to the non-zero radial velocity of the targets (these velocities are reported by WDLS). We then examine in detail the behaviour of the inferred B_ℓ for integration limits (symmetric about the centre-of-gravity of the profile) from several $\mathrm{km\,s^{-1}}$ within the limits of the profile to several $\mathrm{km\,s^{-1}}$ outside the profile limits. The limits are chosen to include all information in the Stokes V profile, but to minimise contributions due to noise outside of the profiles. The selection of the integration limits can therefore be somewhat subjective, but the inferred B_ℓ and net polarisation variations are relatively insensitive to such small differences. Integration limits are shown for each star in Table 1.

Uncertainties associated with each measurement are computed from photon statistical error bars propagated through the reduction of the polarisation spectra and the computation of the LSD profiles, and scaled according to the scheme discussed above.

We have inferred B_ℓ for 14 stars from 129 LSD Stokes V profiles computed by WDLS. The results of these measurements are reported in Sect. 3, and details of individual measurements are provided in Table 2.

2.2 Net linear polarisation measurements

In the context of LSD, net linear polarisation refers to a non-zero equivalent width of the Stokes Q and/or U LSD profiles. This results from differential saturation of the π and σ Zeeman components in all lines used in LSD, i.e. the same phenomenon which is thought to produce broadband linear polarisation.

The net linear polarisation is obtained by computing the normalised equivalent width of the Stokes Q and U LSD profiles. The net Stokes Q is given by:

$$\frac{Q}{I} = \frac{\int Q(v)\, dv}{\int [I_c - I(v)]\, dv}. \tag{2}$$

An analogous expression applies for Stokes U.

Table 1. Stars discussed in this paper, along with ancillary data: HD designation, name, V magnitude, $B-V$ colour index, spectral type, projected rotational velocity, rotational period, the number of longitudinal field measurements obtained, the median longitudinal field uncertainty obtained, the number of net linear polarisation measurements obtained, and the integration limits (blue/red) employed for the measurements.

HD designation	name	m_V	$B-V$	Spectral type	$v\sin i$ (km s^{-1})	P (days)	# B_ℓ	Median σ_B (G)	# net Q/U	Integration limits (km s^{-1})
24712		6.0	+0.32	F0p	6	$12^{\rm d}\!.4610$	4	50		+3/+44
32633		7.1	-0.063	B9p	20	$6^{\rm d}\!.43000$	13	136		-60/+30
40312	θ Aur	2.6	-0.08	A0p	54	$3^{\rm d}\!.61860$	11	33		-33/+102
62140	49 Cam	6.5	+0.26	F0p	23	$4^{\rm d}\!.27679$	14	46	26	-28/+39
65339	53 Cam	6.0	+0.15	A2p	13	$8^{\rm d}\!.02682$	10	78		-46/+39
71866		6.8	+0.09	A2p	14	$6^{\rm d}\!.80022$	10	72		-10/+66
81009		6.5	+0.22	A5p	<5	$33^{\rm d}\!.984$	1	(107)		-22/+63
98088		6.1	+0.20	A3p	33	5.905130	3	44		(SB2)
112185	ϵ UMa	1.8	-0.02	A0p	34	$5^{\rm d}\!.0778$	8	18		-64/+39
112413	α^2 CVn	2.9	-0.12	A0p	14	$5^{\rm d}\!.46939$	18	55	34	-42/+39
118022	78 Vir	4.9	+0.02	A1p	10	$3^{\rm d}\!.7220$	18	41	33	-46/+30
126515		7.1	+0.01	A2p	<3	$129^{\rm d}\!.95$	1	(68)		-42/+34
137909	β CrB	3.7	+0.27	F0p	3.5	$18^{\rm d}\!.4868$	17	21	31	-46/+12
153882		6.3	+0.04	A2p	25	$6^{\rm d}\!.00890$	1	(69)		-69/+8

Leroy (1995a) reported measurements of broadband linear polarisation of several magnetic A and B type stars, obtained using the Sterenn photopolarimeter. It is generally believed that the variable component of broadband linear polarisation is due to non-zero integrated line polarisation induced in strong spectral absorption lines by saturation, and so this quantity is very similar to that obtained using LSD measurements. The broad passband is required simply to build up sufficient polarisation signal for detectability, but (since the effect originates within spectral lines) similar measurements can be obtained by integrating over a small passband, a few lines, or even one single line (or, in our case, LSD profile). On the other hand, the net linear polarisation measured from individual lines should not be expected to have the same numerical value as that measured across a broad passband (although the polarisation angle and relative variation should be similar) because the broadband polarisation is diluted by unpolarised continuum. Therefore, to compare LSD net linear polarisation measurements with those of Leroy (1995a) they will need to be mutually scaled.

Uncertainties associated with each measurement are computed from photon statistical error bars propagated through the reduction process and LSD.

We have inferred net linear polarisation variations for 6 stars in this paper. However, we report only measurements for those 4 stars for which the quality, number and distribution ofobservations provide useful curves of variation. These represent measurements of 124 LSD Stokes Q or U profiles computed by WDLS. The results of the measurements are reported in Sect. 3, and details of individual measurements are provided in Table 3. The integration limits employed were the same as those used for the longitudinal field determinations, and are shown in Table 1.

3 RESULTS FOR INDIVIDUAL STARS

3.1 78 Vir

78 Vir is a fairly sharp-lined A1p star with a moderately strong magnetic field. WDLS report LSD Stokes V, Q and U profiles of 78 Vir at 17 rotational phases, as well as one additional Stokes V observation. We have obtained B_ℓ measurements from each Stokes V profile and net linear polarisation measurements from each Stokes Q and U profile. All measurements have been phased according to the ephemeris of Preston (1969):

$$\mathrm{JD} = 2434816.90 + 3^{\rm d}\!.7220 \cdot \mathrm{E}, \qquad (3)$$

and are reported in Tables 2 and 3.

The phased B_ℓ measurements are shown in Fig. 1 (upper frame), along with B_ℓ measurements obtained by Borra & Landstreet (1980) using a Balmer-line Zeeman analyser. The phased net linear polarisation measurements are shown in Fig. 1 (lower frame), along with broadband linear polarisation measurements reported by Leroy (1995a).

In the case of the B_ℓ measurements, no scaling has been applied to either data set (to be clear, no scaling has been applied to *any* of the longitudinal field measurements discussed in this paper). The agreement between the two sets is clearly satisfactory within the rather large scatter of the measurements by Borra & Landstreet. Superimposed on the measurements is a least-squares first-order Fourier fit to the LSD B_ℓ measurements, for which the reduced χ^2 is 0.61. The value of this statistic for a first-order fit shows that the B_ℓ error bars (the median of which is about 41 G, the smallest being 20 G) do not underestimate the actual scatter about the curve.

The full amplitude of the variation is detected at about the 20σ level. This clear detection, coupled with the long timespan (near one quarter century) between out new longitudinal field measurements and those of Borra & Landstreet (1980), allows for a very high precision determination of the rotational period of this star. An examination of the periodogram of 78 Vir in the region $3^{\rm d}\!.64 - 3^{\rm d}\!.80$ yields the

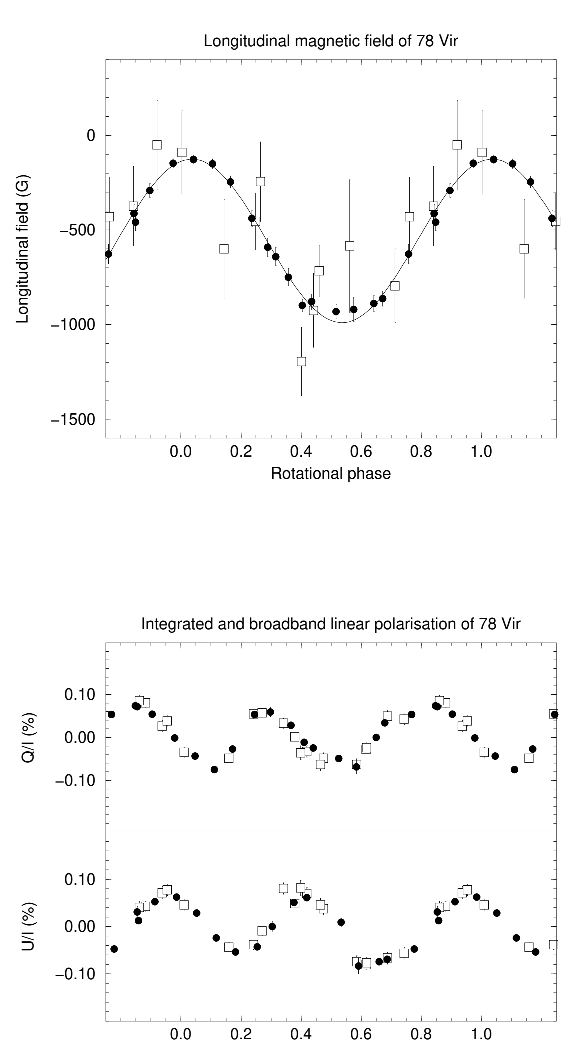

Figure 1. *Upper Frame* - Comparison of mean longitudinal magnetic field measurements B_ℓ obtained from LSD profiles of 78 Vir [solid circles] and those reported by Borra & Landstreet (1980) [open squares]. The curve is a least-squares first-order Fourier fit to the LSD data. *Lower Frame* - Comparison of scaled net linear polarisation measurements obtained from LSD profiles of 78 Vir [filled circles] and the broadband linear polarisation measurements of Leroy (1995a) [open squares]. 1σ error bars accompany each data point in both frames.

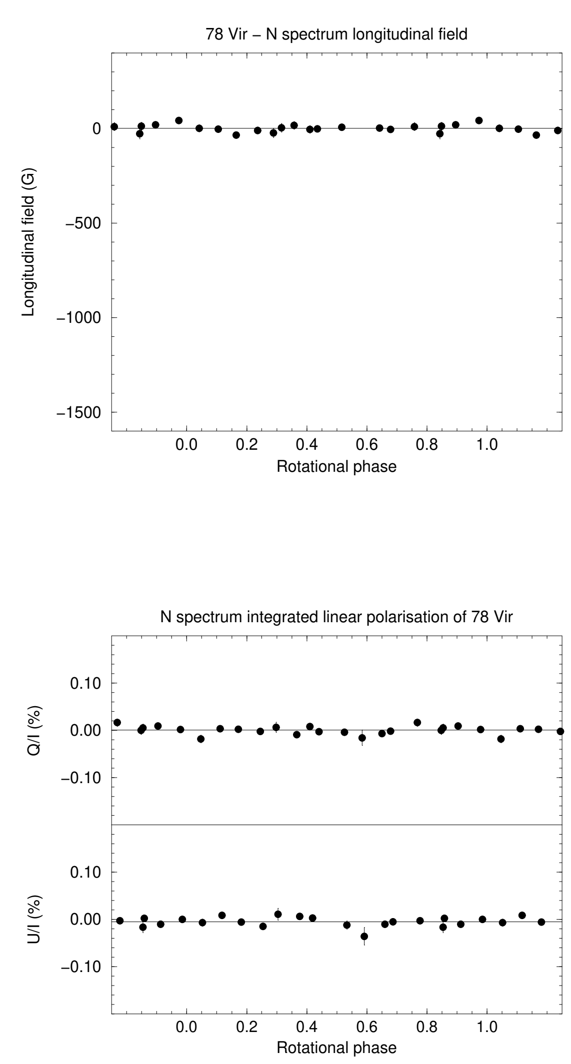

Figure 2. *Upper Frame* - Mean longitudinal magnetic field B_ℓ of 78 Vir measured from the null (N) spectra associated with Stokes V. *Lower Frame* - Net linear polarisation as measured from the N spectra associated with Stokes Q and U. The solid lines show the mean of each data set.

the period $P_{rot} = 3\overset{\rm d}{.}72203 \pm 0\overset{\rm d}{.}00023$. This period is consistent with $P_{\rm rot} = 3\overset{\rm d}{.}722084 \pm 0\overset{\rm d}{.}000042$ reported by Catalano & Leone (1994). The combined longitudinal field data are however only barely consistent, and the photometric observations of Catalano & Leone are not consistent, with a period of $3\overset{\rm d}{.}7218$, the period which Leroy (1999, priv. comm.) informs us is crucial in order to obtain the stable magnetic field model consistent with the broadband linear polarisation described by Leroy et al. (1996). As this period is not admitted by the photometric data (and probably not admitted by the magnetic data), the magnetic field of 78 Virginis likely exhibits very strong departures from a dipolar configuration (Leroy 1999, priv. comm.). This important conclusion is discussed in more detail by WDLS.

The net linear polarisation measurements, on the other hand, must be both shifted and scaled to usefully compare the two data sets. First, we have subtracted from each of the measurements (both broadband and LSD) the zeroth-order term in a third-order Fourier fit (i.e. a Fourier expansion up to and including the $\cos 3\phi$ and $\sin 3\phi$ terms) to their respective variations. In the case of the broadband measurements this term potentially includes contributions from interstellar polarisation and Zeeman effect, while in the case of the LSD measurements this term should result solely from Zeeman effect. We remove this zeroth-order term from both sets to compare the variable component. Secondly, the LSD Stokes Q and U measurements (and error bars) of 78 Vir have been scaled by a factor of 0.10 to achieve the best agreement with the broadband data. The motivation for this scaling was discussed in the previous Section.

The net broadband and LSD linear polarisation variations agree extremely well with those reported by Leroy (1995a). There is no suggestion of systematic differences between the two sets of measurements. This is remarkable; given that the broadband and LSD data are obtained using very different methods, it would not be surprising to find small systematic differences in the shapes of the variations. Our net linear polarisation measurements are obtained from *direct integration* of the Zeeman linear polarisation within spectral lines. We can therefore confirm, based on the exceptionally good agreement between the LSD and broadband net linear polarisation variations, that the broadband linear polarisation measured with photoelectric polarimeters is in fact produced by saturated linear polarisation within Zeeman-split spectral lines. The reduced χ^2s of least-squares third-order Fourier fits to the combined Stokes Q and U measurements (solid curves) are respectively 2.2 and 1.3. These values of the reduced χ^2 statistic are consistent with the LSD error bars.

As discussed in Sect. 2, one of this procedure is the generation of a diagnostic null (or N) spectrum associated with each Stokes V, Q or U observation. Because N is computed using subexposures acquired with identical instrument or waveplate orientations it should nominally show no detectable signal, and should therefore provide a accurate indication of the noise. Additionally, the presence of a detectable signal in N indicates a spurious contribution and allows us to diagnose the degree of contamination of the observations. In Fig. 2 we show (upper frame) B_ℓ as measured from the Stokes V null spectrum, and (lower frame) the net linear polarisation as measured from the Stokes Q and U null spectra. One should note the following: (1) No systematic variations are detected in the Stokes V, Q or U nulls, indicating that any variable spurious contribution to the longitudinal field or net linear polarisation variations shown in Fig. 1 are below the detection threshold; (2) The mean is consistent with zero (1σ) in all 3 cases, indicating that any systematic baseline contribution is below the detection threshold; and (3) the reduced χ^2s of the V, Q and U data about their means are respectively 1.3, 1.5 and 1.6. Therefore the adopted error bars are consistent with the scatter about the means. This indicates that the N spectrum error bars (which are never scaled) are consistent with the true associated uncertainties. One should note that the error bars obtained from B_ℓ measurements of the N spectra (associated with Stokes V) are systematically smaller (by factors from about 1.5 to 3.0) than those obtained from measurements of B_ℓ from the V spectra themselves due to the scaling described in Sect. 2. Similar results for N have been obtained for all other stars studied in this paper.

3.2 β CrB

β CrB is a sharp-lined F0p star with a moderately strong field. WDLS reported LSD Stokes V, Q and U profiles of β CrB at 16 rotational phases, as well as one additional Stokes V observation. We have obtained B_ℓ measurements from each Stokes V profile and net linear polarisation measurements from each Stokes Q and U profile. All measurements have been phased according to the ephemeris of Kurtz (1989):

$$\mathrm{JD} = 2434204.70 + 18.^{\rm d}4868 \cdot \mathrm{E}, \quad (4)$$

and are reported in Tables 2 and 3.

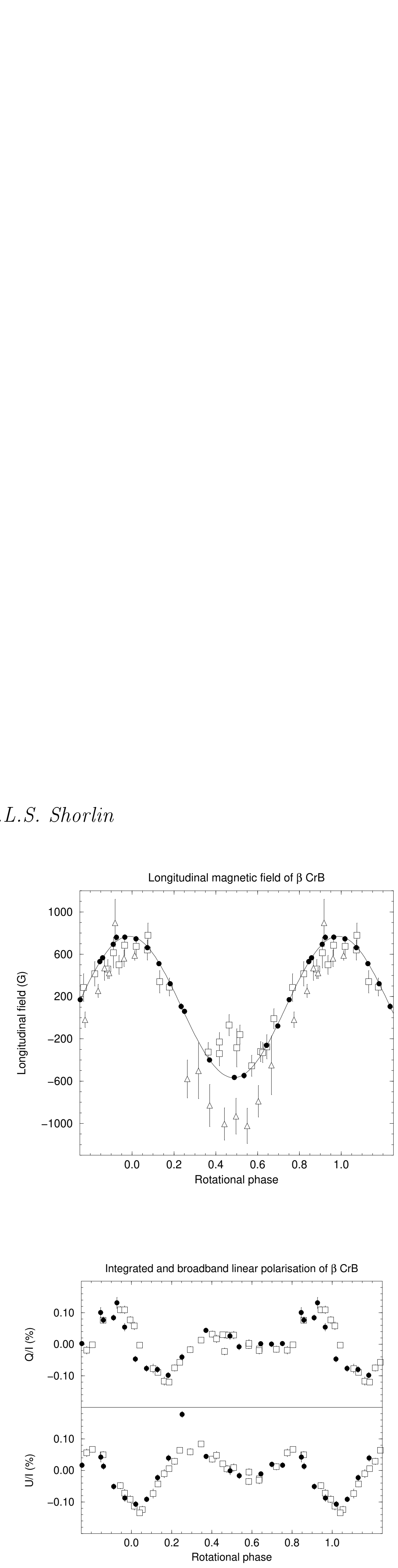

Figure 3. *Upper Frame* - Comparison of mean longitudinal magnetic field measurements B_ℓ obtained from LSD profiles of β CrB [solid circles], those reported by Borra & Landstreet (1980) [open squares], and those reported by Mathys (1991) and Mathys & Hubrig (1997) [open triangles]. The solid curve is a least-squares first-order Fourier fit to the LSD measurements. *Lower Frame* - Comparison of scaled net linear polarisation measurements obtained from LSD profiles of β CrB [filled circles] and the broadband linear polarisation measurements of Leroy (1995a) [open squares]. 1σ error bars are provided.

The LSD B_ℓ measurements are compared with those published previously by Borra & Landstreet (1980) and Mathys (1991)/Mathys & Hubrig (1997) in Fig. 3 (upper frame). The LSD measurements (which have a median 1σ uncertainty of about 21 G, and the smallest of which is 16 G) agree with those of Borra & Landstreet, apart from the fact that the LSD data do not show the hump near magnetic minimum visible in the Balmer-line Zeeman analyser data. The agreement with those of Mathys/Mathys & Hubrig is considerably poorer, there being both a difference in amplitude and mean between the two variations (note that the measurements of Mathys (1991) seem to disagree in this respect with almost *all* other determinations of the longitudinal field variation of this star; see the discussion by Mathys [1991]). Such differences in the longitudinal field variations may hint at nonuniform chemical abundance distributions which are not detectable in the Stokes I profiles of β CrB due to the slow rotation and low axial inclination. The solid curve in Fig. 2 (upper frame) is a least-squares first-order Fourier fit to the LSD measurements. The reduced χ^2 is 0.35, indicating that departures from a pure sinusoidal B_ℓ variation must be very small, perhaps surprising given the important phase shift between the longitudinal field and field modulus extrema (Mathys et al. 1997), suggesting a highly non-dipolar field configuration (e.g. Leroy 1995b). The longitudinal field variation is detected at the 66σ level.

The LSD net linear polarisation measurements are compared with those published by Leroy (1995a) in Fig. 2 (lower frame). The LSD linear polarisation measurements have been scaled by a factor of 0.28, and we have subtracted from all measurements the appropriate zeroth-order term from least-squares third-order Fourier fits. The agreement between the two data sets is satisfactory, although not quite as good as in the case of 78 Vir. This may indicate that small systematic differences exist between the LSD and broadband net linear polarisation variations of β CrB. Note in particular the very strong Stokes U datum near phase 0.25. The U and N profiles associated with this measurement appear altogether normal (see WDLS), and suggest that real differences exist between the broadband and LSD net polarisation variations. In addition, a phase shift of about 0.02 cycles between the LSD and broadband variations in both Stokes Q and U appears to be present in Fig 2 (lower frame). Our first interpretation of this shift was that that it results from a period error. However, because the broadband and LSD measurements were obtained less than 3 years apart, this shift translates into a period error of $0.^{\rm d}01$. This is far greater than the error associated with the period of this star ($18.^{\rm d}4868 \pm 0.^{\rm d}0006$; Kurtz 1989), and is anyhow not consistent with the new B_ℓ measurements considered along with those of Borra & Landstreet (1980; which together constrain the period to $18.^{\rm d}4868 \pm 0.^{\rm d}005$). The apparent shift is therefore not due to a period error. It may simply be illusory, impressed by the arrangement of 1 or 2 data points near phase 0.0 which are plotted twice in these 1.5-cycle phase diagrams (and may reinforce the impression of a systematic trend where none exists). However, if these differences are real they could be an indication of axial precession (Adelman 1999; Shore & Adelman 1976). Third-order least-squares Fourier fits achieve rather high reduced χ^2s of 4.8 and 5.8 for the Q and U variations respectively.

3.3 53 Cam

53 Cam is a fairly sharp-lined A2p star with a strong field. WDLS reported LSD Stokes V, Q and U profiles of 53 Cam at 9 rotational phases, as well as one additional Stokes V observation. We have obtained B_ℓ measurements from each Stokes V profile, and net polarisation measurements from the Stokes Q and U profiles. All measurements have been phased according to the ephemeris of Hill et al. (1998):

$$\mathrm{JD} = 2448498.186 + 8.^{\rm d}02681 \cdot \mathrm{E}, \quad (5)$$

and the B_ℓ data are reported in Table 2.

In Fig. 4 (upper frame) we compare the LSD B_ℓ measurements with B_ℓ measurements obtained using a Balmer-line Zeeman analyser, published previously by Hill et al. (1998). The agreement is clearly quite good. However, if we attempt to fit the LSD B_ℓ measurements by least-squares with a first-order Fourier fit (dashed curve), the resultant reduced χ^2 is 20.5. On the other hand, the reduced χ^2 of a third-order Fourier fit is 0.2 (solid curve; the fit for a second-order fit, with $\chi^2/\nu = 14.4$, is not much better than that of first order). It is clear in Fig. 4 (upper frame) that the third-order fit is systematically different than that of first order; i.e. it is not simply fitting scatter larger than that implied by the error bars. We therefore unambiguously detect non-sinusoidal contributions to the LSD longitudinal field variation of 53 Cam, which are not visible in the Hβ curve and which could very well be due to abundance inhomogeneities (see for example Landstreet 1988). We have searched for the effects of such inhomogeneities on the longitudinal field variation by performing a differential analysis using Fe, Cr and Ti line masks. The longitudinal field variations as measured from Fe and Cr lines (Fig. 4, lower frame) are effectively identical to that found from the combined analysis shown in Fig. 4 (upper frame). The Ti B_ℓ curve, on the other hand, is strikingly different from the others, particularly around phase 0.25 when the positive magnetic pole is in view. While the Fe and Cr curves show a strong positive B_ℓ at this phase, the Ti curve is consistent with a null field. This likely results from the near-disappearance of the Ti mean line near magnetic maximum (WDLS), implying that Ti is strongly underabundant at the positive pole (consistent with the results of Landstreet 1988). Thus Ti does not sample the positive magnetic pole, the surface region which contributes almost all of the circular polarisation (i.e. longitudinal field) near phase 0.25. This is consistent with the important differences observed by WDLS between the Fe and Ti Zeeman signatures of 53 Cam.

The median uncertainty of the LSD B_ℓ measurements of 53 Cam (those obtained using all lines) is 78 G. The median uncertainties obtained for the differential measurements are poorer than those obtained from the full analysis (110 G for Fe, 138 G for Cr, and about 600 G for Ti). While increase in the size of the median error bar for Fe and Cr are very close to that predicted due to the decrease in the number of lines employed (WDLS; i.e. a decrease in precision as the square root of the number of lines), the median error bar for Ti is about 2 times worse than that predicted. As Ti lines only account for some 6% of all lines in the A2p mask (WDLS), we speculate that this results from a rapid increase in the size of the deconvolution errors as the number of lines decreases.

Our measurements of the net linear polarisation of 53 Cam, on the other hand, are considerably less satisfactory than those obtained for 78 Vir and β CrB. Straight-line fits to the phased Q and U net polarisation variations achieve respective reduced χ^2s of 1.6 and 1.0; clearly the scatter is consistent with random errors, and no variation is detected. This results from two sources: First, the S/N of the 53 Cam spectra obtained by WDLS is uniformly low, typically un-

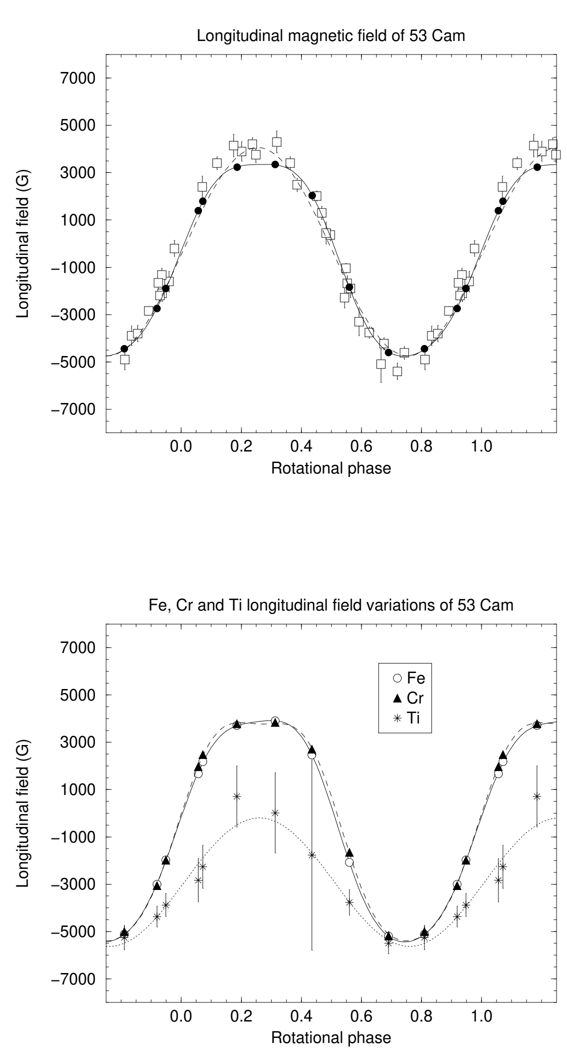

Figure 4. *Upper frame* – Longitudinal magnetic field variation of 53 Cam. *Open squares* – Hβ B_ℓ measurements by Hill et al. (1998). *Filled circles* – B_ℓ from this work, computed from LSD Stokes V profiles (WDLS). The dashed curve is a first-order Fourier series fit to the LSD measurements by least-squares (χ^2/ν = 20.5), the solid curve a Fourier series of third order (χ^2/ν = 0.2). *Lower frame* – Longitudinal magnetic field variations for Fe [open circles], Cr [filled triangles] and Ti [asterisks]. The curves are third-order [Fe, Cr] and first-order [Ti] Fourier fits. 1σ error bars are provided.

der 200:1. Secondly, an examination of the LSD Stokes Q and U profiles of 53 Cam reported by WDLS reveals an important difference with respect to those reported for 78 Vir: the profiles of 78 Vir are nearly always either entirely positive, or entirely negative. Therefore integration across the profile to obtain the net polarisation almost always yields a substantial signal. In the case of 53 Cam, the profiles are significantly more complex, and are *never* entirely positive or entirely negative. Integration across the profiles of 53 Cam results in destructive cancellation of positive signal by negative signal, and yields a small net polarisation. While the linear polarisation profiles of β CrB also exhibit positive and negative components, the S/N of those profiles is so high that net polarisation is still detected. In any case, our net polarisation measurements are consistent with the results of Leroy (1995a) who finds the broadband linear polarisation variation of this star to be highly complex and of very low amplitude.

3.4 α^2 CVn

α^2 CVn is a fairly sharp-lined A0p star with a moderately strong magnetic field. WDLS reported LSD Stokes V, Q and U profiles of α^2 CVn at 18 rotational phases. We have obtained B_ℓ measurements from each Stokes V profile, and net linear polarisation measurements from each Stokes Q and U profile. All the B_ℓ measurements have been phased according to the ephemeris of Farnsworth (1932):

$$\mathrm{JD} = 2419869.720 + 5.^{\mathrm{d}}46939 \cdot \mathrm{E}, \qquad (6)$$

and are reported in Tables 2 and 3.

The phased B_ℓ measurements are shown in Fig. 4 (upper frame), along with those reported by Borra & Landstreet (1977; obtained using a Balmer-line Zeeman analyser) and those reported by Landstreet (1982; obtained using a coudé line profile scanner at Fe II 492.3 nm). Also shown are a first-order least-squares Fourier fit to the Borra & Landstreet measurements (dashed curve) and a second-order Fourier fit to the LSD measurements (solid curve, χ^2/ν=1.2). The agreement between the LSD and the metallic-line measurements is quite good, although the LSD measurements may show a slightly lower field at magnetic maximum. On the other hand, the agreement between the LSD and Balmer-line Zeeman analyser variations is clearly not very good, especially near magnetic minimum. This is not surprising; in addition to Landstreet's measurements and the LSD measurements reported here, we find other reports of the longitudinal field variation derived from metallic line measurements (Babcock 1952; Pyper 1969) to be strongly discrepant with respect to the Balmer-line Zeeman analyser measurements. These differences probably result from the very important abundance nonuniformities (most remarkably Fe) found in the atmosphere of this star. WDLS show that important differences exist between the shapes of the Fe and Cr line Zeeman signatures of α^2 CVn. As in the case of 53 Cam, this effect is also visible in measurements of the longitudinal field. In Fig. 5 (lower frame) we show B_ℓ measurements of α^2 CVn obtained using lines of Fe (open circles) and lines of Cr (filled triangles). There is a clear difference in amplitude (more than a factor of two) and in shape, as well as a shift in phase. In this Figure we also show Landstreet's (1982) measurements. Because these measurements were obtained using a line of Fe, they should be compared with the LSD B_ℓ measurements from Fe lines. The agreement is excellent; note in particular that the field strength at magnetic maximum as measured using Fe LSD profiles agrees very well with Landstreet's coudé result. This comparison represents perhaps the most demanding test of the accuracy of LSD B_ℓ measurements. The median uncertainty associated with the LSD longitudinal field measurements (those computed using all lines) is 55 G (about one half the median uncertainty of the measurements reported by Borra & Landstreet), while the best measurement has an error bar of 41 G. The longitudinal field variation is detected at about the 25σ level. The median uncertainties associated with the Fe and Cr B_ℓ mea-

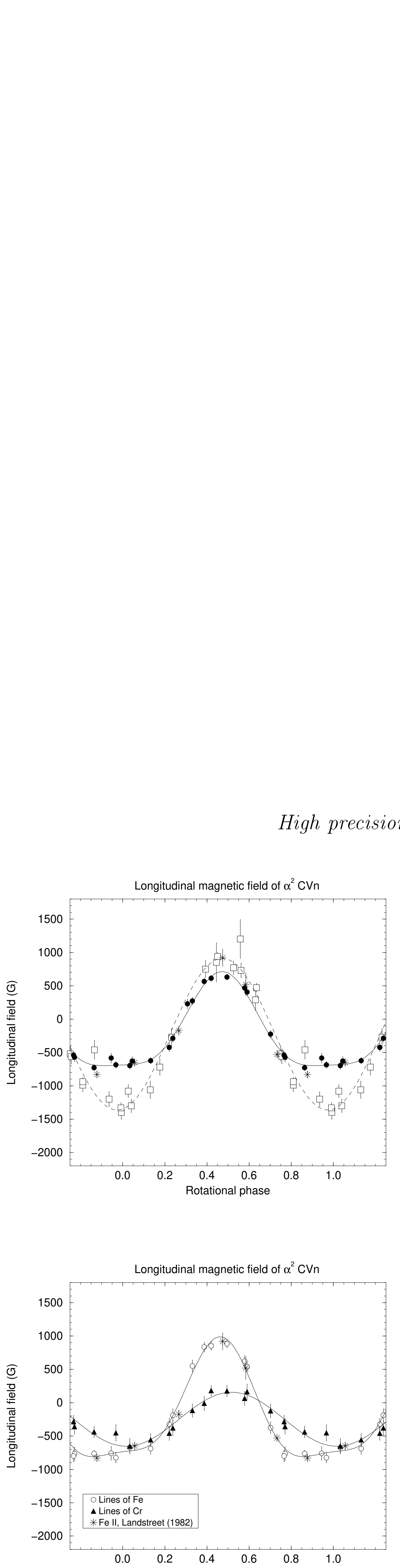

Figure 5. *Upper frame* – Comparison of mean longitudinal magnetic field measurements B_ℓ obtained from LSD profiles of α^2 CVn [solid circles], those reported by Borra & Landstreet (1977) [open squares], and those obtained by Landstreet (1982) [asterisks]. *Lower frame* – Comparison of LSD mean longitudinal magnetic field measurements B_ℓ of α^2 CVn obtained from Fe lines [open circles] with those obtained from Cr lines [filled triangles]. The curves are least-squares second-order [Fe lines] and first-order [Cr lines] Fourier fits.

surements are poorer (Fe: 81 G; Cr: 104 G), due to the use of fewer lines in the differential analyses. The increases in the median uncertainties are consistent with those expected from the line frequencies published by WDLS for an A0p line mask.

An examination of the linear polarisation profiles of α^2 CVn reported by WDLS shows them to be qualitatively similar to those of 78 Vir: the profiles are often entirely positive or entirely negative, and therefore should produce a coherent net polarisation signal. This prediction is borne out; the phased net linear polarisation variations of α^2 CVn are shown in Fig. 6, both versus phase and versus one another, accompanied by fourth-order least-squares Fourier fits (with reduced χ^2s of 0.8 for Stokes Q and 8.3 for Stokes U). The net linear polarisation of α^2 CVn has previously been investigated by Kemp & Wolstencroft (1974). They found that both the narrowband and broadband polarisations of this star are extremely small. While the precision of their broadband measurements (obtained in the red, blue and UV) is impressive (typically 3×10^{-5}), no convincing variation of either Stokes Q or U was obtained. However, the polarisation within a narrow band centred on Hβ is slightly stronger, and a reasonably clear (although noisy) variation was obtained (details of individual measurements were not provided, and so we are unable to show those measurements here). This variation (shown in Fig. 7 of Kemp & Wolstencroft 1974) is quite consistent with the data published here. We confirm the suspicion of Kemp & Wolstencroft that the variation in the Q-U plane implies a clockwise rotation of the star as seen projected upon the sky. We furthermore apply the method described by Leroy et al. (1995a) to obtain an unambiguous (although undoubtably highly simplified) model of the magnetic field geometry of α^2 CVn. When considered along with the B_ℓ measurements of Borra & Landstreet (1977), the linear polarisation data imply a rotational axis inclination $i = 118^\circ$ and magnetic axis obliquity $\beta = 72^\circ$, with uncertainties of about 5° for each angle. As is discussed by Leroy et al. (1995a), the inclination $i > 90^\circ$ specifies the clockwise rotation of the polarisation diagramme, and therefore the clockwise rotation of the star as seen projected on the sky. If we assume that the dipole is centred, we obtain a polar strength $B_{\rm d} = 4.5$ kG. These results are reasonably similar to the centred dipole model described by Borra & Landstreet (1977).

3.5 49 Cam

49 Cam is a fairly broad-lined F0p star with a moderately strong magnetic field. WDLS reported LSD Stokes V, Q and U profiles of 49 Cam at 13 rotational phases, as well as one additional Stokes V observation. We have obtained B_ℓ measurements from each Stokes V profile, and net polarisation measurements from each Stokes Q and U profile.

All measurements have been phased according to the ephemeris of Adelman (1997a):

$$\mathrm{JD} = 2441257.300 + 4\overset{\mathrm{d}}{.}28679 \cdot \mathrm{E}, \qquad (7)$$

and are reported in Tables 2 and 3.

The phased LSD B_ℓ measurements of 49 Cam are shown in Fig. 7 (upper frame), along with unpublished measurements obtained by the authors using a Balmer-line Zeeman analyser. Also shown are first- and second-order least-squares Fourier fits to the LSD measuremements, the respective reduced χ^2s of which are 3.0 and 1.4. The factor-of-two improvement in this statistic for a second-order fit suggests that mild nonsinusoidal contributions may be detected. The agreement between the LSD and Balmer-line Zeeman analyser datasets is very good. The median uncertainty associated with the B_ℓ measurements is about 46 G, and the smallest uncertainty is 37 G. This should be compared with the Balmer-line Zeeman analyser measurements, which have typical uncertainties around 500 G (i.e. more than one order of magnitude larger). The longitudinal field variation is detected at about the 65σ level.

The measurements errors associated with the LSD net linear polarisation data are in general comparable to those

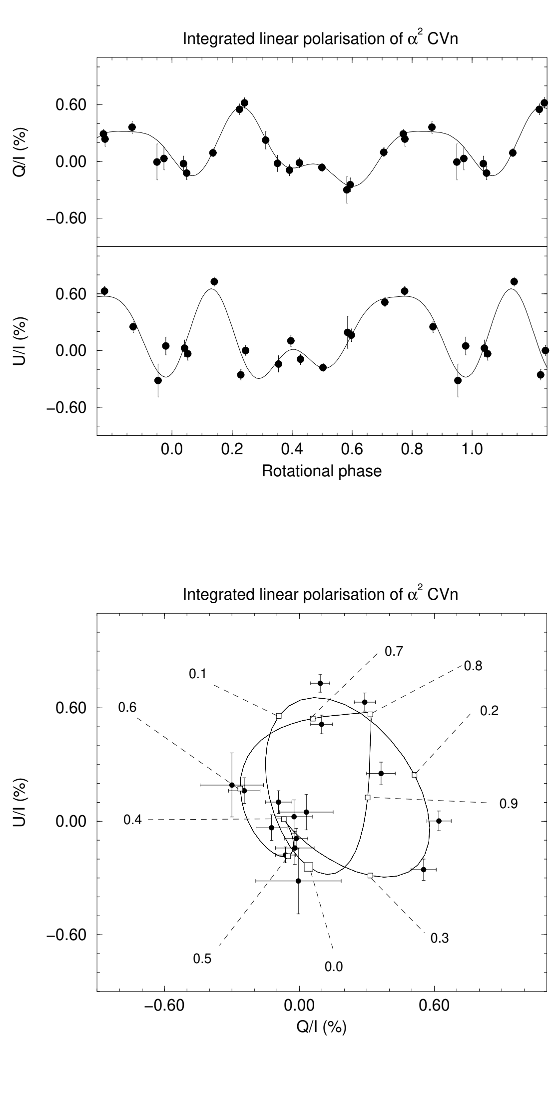

Figure 6. Net linear polarisation variation of α^2 CVn, measured from the LSD Stokes Q and U profiles. The solid curves are least-squares $4^{\rm th}$-order Fourier fits. Phases are indicated in the lower frame.

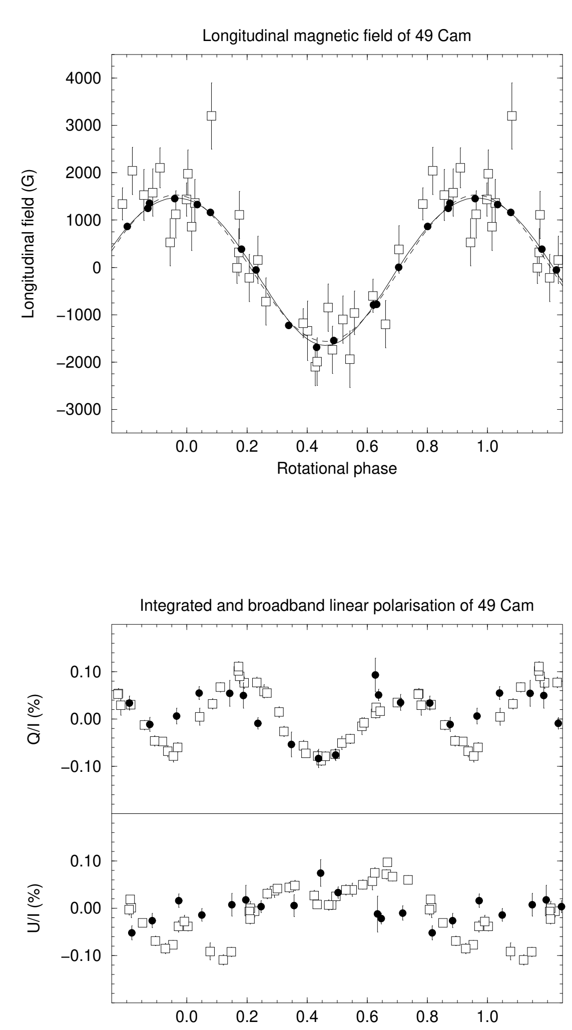

Figure 7. *Upper Frame* - Comparison of mean longitudinal magnetic field measurements B_ℓ obtained from LSD profiles of 49 Cam [solid circles] and unpublished Hβ measurements obtained by the authors [open squares]. The dashed curve is a first-order Fourier fit to the LSD measurements, while the solid curve is a second-order Fourier fit to the LSD measurements. *Lower Frame* - Comparison of scaled net linear polarisation measurements obtained from LSD profiles of 49 Cam [filled circles] and the broadband linear polarisation measurements of Leroy (1995a) [open squares]. 1σ error bars are provided.

obtained using broadband polarimetry. The LSD measurements are compared with the broadband data reported by Leroy (1995a) in Fig. 7 (lower frame). The Q and U profiles reported by WDLS are qualitatively similar to those reported for 53 Cam: complex, and almost never confined to entirely negative or positive polarisation across the line. We attribute the relatively high quality of these net polarisation measurements to the later spectral type of the star, and hence higher S/N of the 49 Cam LSD profiles. While the LSD Stokes Q net polarisation variation is similar to that reported by Leroy (1995a), the U variations do not agree very well. This provides additional evidence for real differences between LSD and broadband net polarisation variations. The net polarisation measurements have been scaled by a factor of 0.14.

3.6 HD 32633

HD 32633 is a fairly broad-lined B9p star with a strong, non-axisymmetric magnetic field. WDLS reported LSD Stokes V, Q and U profiles of HD 32633 at 12 rotational phases, as well as one additional Stokes V observation. We have obtained B_ℓ measurements from each Stokes V profile, and also net linear polarisation measurements from the Stokes Q and U profiles. The data have been phased according to the ephemeris of Adelman (1997b):

$$\mathrm{JD} = 2437635.200 + 6.^{\rm d}43000 \cdot \mathrm{E}, \qquad (8)$$

and the B_ℓ measurements are reported in Table 2.

The phased B_ℓ measurements are shown in Fig. 8, along

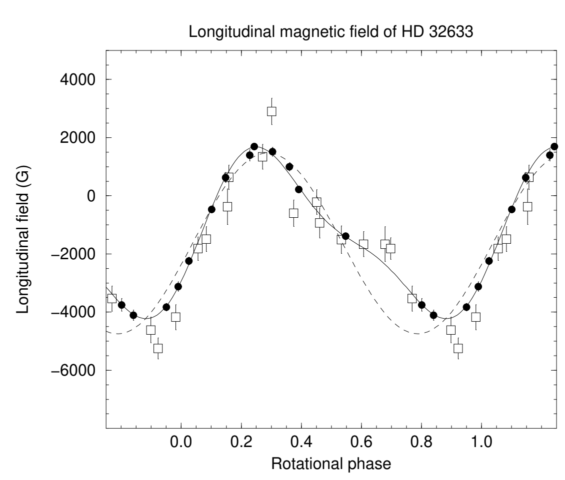

Figure 8. Mean longitudinal magnetic field variations of HD 32633. B_ℓ as measured from LSD Stokes V profiles [Filled circles], B_ℓ from Borra & Landstreet (1980) [Open squares]. The solid and dashed curves are respectively second-order and first-order least-squares Fourier fit to the LSD measurements. 1σ error bars are provided.

with measurements published previously by Borra & Landstreet (1980). Also shown are second-order and first-order least-squares Fourier fits to the LSD measurements, which have respective reduced χ^2s of 0.98 and 20.3. The strong departures from a sinusoidal variation, first reported by Borra & Landstreet (1980) and confirmed by Renson (1984), are clearly visible in both the LSD and Balmer-line Zeeman analyser curves. The median uncertainty associated with the LSD measurements is about 136 G, while the best measurement has an error bar of 56 G. This should be compared to the measurements of Borra & Landstreet, for which the typical uncertainty is about 450 G, and for which the best uncertainty is 365 G. The variation is detected at about the 50σ level.

The LSD Stokes Q and U profiles obtained for HD 32633 by WDLS are of rather low S/N. No Stokes U net polarisation variation is detected, while that of Stokes Q is detected only marginally. These net polarisation data are too noisy to add anything of value to our understanding of the magnetic field of HD 32633. Leroy (1995a) was also unable to detect broadband polarisation variation in the spectrum of this star. As WDLS clearly detect LSD linear polarisation signatures in the spectral lines of HD 32633, this emphasises that integrated quantities such as net linear polarisation are limited in their ability to characterise stellar magnetic fields.

3.7 HD 71866

HD 71866 is a fairly sharp-lined A2p star with a moderately strong field. WDLS reported LSD Stokes V, Q and U profiles of HD 71866 at 9 rotational phases, as well as one additional Stokes V observation. We have obtained B_ℓ measurements from each Stokes V profile and net linear polarisation measurements from each Stokes Q and U profile. The B_ℓ data, along with measurements published previously by

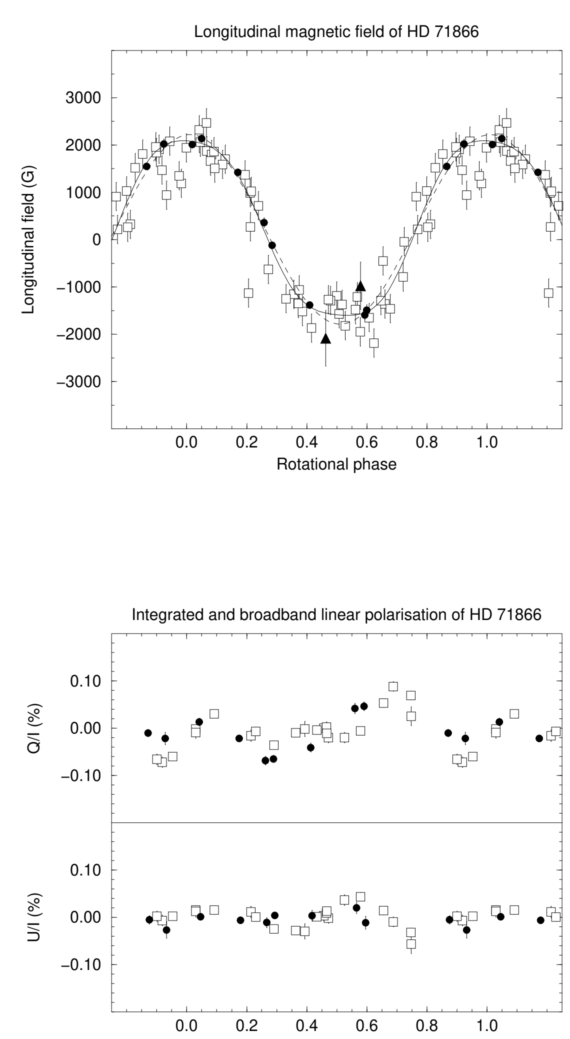

Figure 9. *Upper Frame* - Comparison of mean longitudinal magnetic field measurements B_ℓ obtained from LSD profiles of HD 71866 [solid circles], unpublished Hβ measurements obtained by the authors [solid triangles] and measurements reported by Babcock (1958) [open squares]. The solid curve and dashed curves are respectively least-squares third-order and first-order Fourier fits to the LSD measurements. *Lower Frame* - Comparison of scaled net linear polarisation measurements obtained from LSD profiles of HD 71866 [filled circles] and the broadband linear polarisation measurements of Leroy (1995a) [open squares]. 1σ error bars are provided.

Babcock (1956; with assumed error bars of 250 G) and unpublished Balmer-line Zeeman analyser measurements obtained recently by the authors, have been phased according to the ephemeris of Bagnulo et al. (1995a):

$$\mathrm{JD} = 2438297.5 + 6.^{\rm d}80022 \cdot \mathrm{E}. \quad (9)$$

The phased measurements are reported in Table 2.

In Fig. 9 (upper frame) we show the new B_ℓ measurements, along with those of Babcock (1956) and the unpublished Balmer-line Zeeman analyser measurements, phased according to the ephemeris cited above. Also shown is a first-order least-squares Fourier fit (dashed curve) to the

LSD measurements, the reduced χ^2 of which is 2.6. A third-order Fourier fit (solid curve) achieves a much improved reduced χ^2 of 1.2, and may suggest flattened extrema in the B_ℓ curve. The median of the measurement error bars is about 72 G, and the best measurement has an error bar of 63 G. The variation is detected at about the 54σ level. Note that the combined B_ℓ measurements are not consistent with the $6^{\mathrm{d}}_{.}80054 \pm 0^{\mathrm{d}}_{.}00002$ period reported by Catalano & Leone (1990). This period results in a significant phase shift between Babcock's data and that obtained recently (i.e. the unpublished Hβ data and the data reported herein).

In Fig. 9 (lower frame) we compare the LSD net linear polarisation measurements with broadband polarisation measurements obtained by Leroy (1995a). Both data sets have been phased according to the ephemeris described above. A scaling factor of 0.07 brings the LSD and broadband measurements into approximate agreement. This may indicate that differences exist between the LSD and broadband linear polarisation variations of HD 71866.

3.8 HD 24712

HD 24712 is a sharp-lined F0p star with a moderately strong field. WDLS obtained 4 Stokes V, Q and U observations of this star. We have computed B_ℓ from the Stokes V LSD profiles, and report these values in Table 2. The number of LSD linear polarisation signatures obtained by WDLS is insufficient to derive the net polarisation variation.

We first combined our new B_ℓ measurements of HD 24712 with the Hβ magnetometer data obtained by Ryabchikova et al. (1997) and phased the combined set according to the $12^{\mathrm{d}}_{.}4610$ period of Mathys & Hubrig (1997). A phase difference is evident between the two data sets, and accordingly the best-fit sinusoid to the combined set achieves a rather poor reduced χ^2 of 5.1. We then computed the phase assuming the ephemeris of Kurtz & Marang (1987):

$$\mathrm{JD} = 2440577.230 + 12^{\mathrm{d}}_{.}4572 \cdot \mathrm{E}. \qquad (10)$$

When the combined data are phased according to this ephemeris their mutual agreement is much better, and a least-squares sine fit achieves a reduced χ^2 of 2.0. When Mathys & Hubrig's (1997) CASPEC/Balmer-line Zeeman analyser observations are phased according to this period, a large systematic difference is observed between these data and the LSD/Hβ combined set. A very similar difference is also evident in Fig. 1 of Mathys & Hubrig (1997) where those data are compared to measurements obtained by Preston (1972). We therefore conclude (1) that the ephemeris of Kurtz & Marang (1987) provides a good description of all modern data, while that of Mathys & Hubrig (1997) does not; and (2) that a large systematic offset exists between the observations of Mathys & Hubrig (1997) and all other available longitudinal field measurements, including those reported here. All three data sets are shown in Fig. 10.

When the phased LSD B_ℓ measurements alone are fit by least-squares with a first-order Fourier series the reduced χ^2 is 0.66. This fit is also shown in Fig. 10. The median LSD B_ℓ uncertainty obtained for HD 24712 is about 50 G, the best measurement has an error of 42 G, and the variation is detected at about the 25σ level.

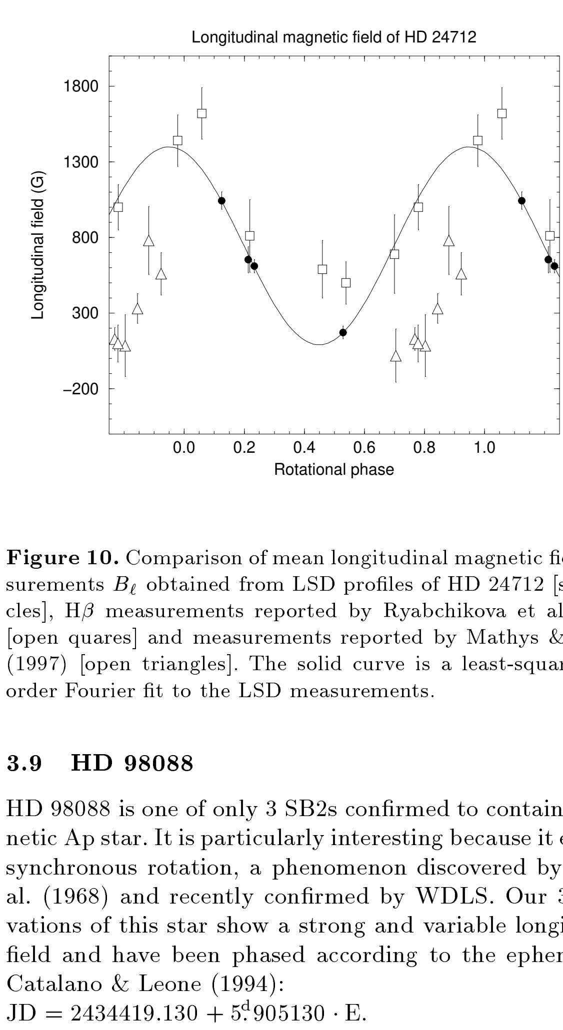

Figure 10. Comparison of mean longitudinal magnetic field measurements B_ℓ obtained from LSD profiles of HD 24712 [solid circles], Hβ measurements reported by Ryabchikova et al. (1997) [open quares] and measurements reported by Mathys & Hubrig (1997) [open triangles]. The solid curve is a least-squares first-order Fourier fit to the LSD measurements.

3.9 HD 98088

HD 98088 is one of only 3 SB2s confirmed to contain a magnetic Ap star. It is particularly interesting because it exhibits synchronous rotation, a phenomenon discovered by Abt et al. (1968) and recently confirmed by WDLS. Our 3 observations of this star show a strong and variable longitudinal field and have been phased according to the ephemeris of Catalano & Leone (1994):

$$\mathrm{JD} = 2434419.130 + 5^{\mathrm{d}}_{.}905130 \cdot \mathrm{E}. \qquad (11)$$

These data agree quite well with those reported by Babcock (1958), which have been phased according to the ephermeris cited above and are shown together in Fig. 11. The dashed curve in Fig. 11 is a least-squares first-order Fourier fit to Babcock's measurements. Note that at some phases the mean profiles of the primary and secondary star were blended, and that the line of the secondary may affect the longitudinal field determination at a low level. While the number of LSD measurements is limited, the 14σ difference between the LSD measurement at phase 0.183 and those reported by Bonsack (1976) near this phase suggests that serious inconsistencies exist between the LSD measurements and those of Bonsack (1976). This is consistent with the important differences we observe between the measurements of Babcock (1958) and those of Bonsack (1956) as well.

3.10 θ Aur

θ Aur is a broad-lined A0p star with a weak magnetic field. WDLS obtained LSD Stokes V profiles of θ Aur at 11 rotational phases. We have obtained B_ℓ measurements from each Stokes V profile. When the new measurements, along with those reported by Borra & Landstreet (1980), are phased according to the $3^{\mathrm{d}}_{.}6188$ period reported by Adelman (1997a), a small (0.1 cycles) phase shift is apparent between the two data sets. Assuming that this results from a period error, we

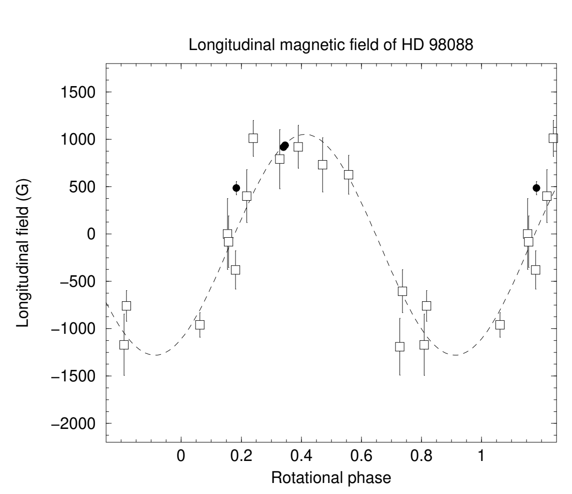

Figure 11. Comparison of mean longitudinal magnetic field measurements B_ℓ obtained from LSD profiles of HD 98088 [solid circles] and measurements reported by Bonsack (1976) [open squares]. The solid curve is a least-squares first-order Fourier fit to Bonsack's measurements.

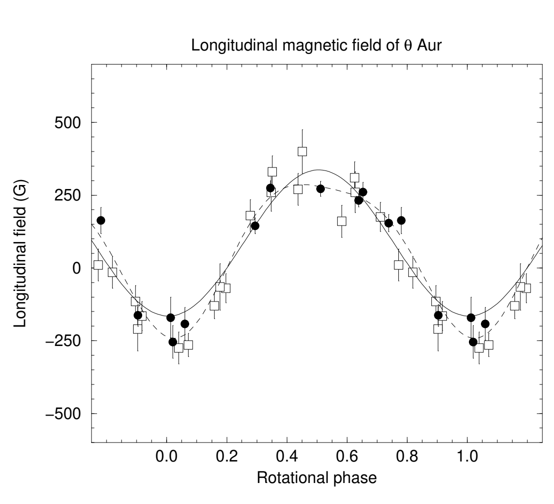

Figure 12. Comparison of the longitudinal magnetic field measurements B_ℓ of θ Aur obtained from LSD profiles [solid circles] and Hβ measurements by Borra & Landstreet (1980) [Open Squares]. Measurements are phased according to the ephemeris discussed in the text. The curves are first-order [dashed] and second-order [solid] least-squares Fourier fits to the LSD measurements. 1σ error bars are provided.

can search the periodogram for improved periods near $3^{\rm d}_{\cdot}618$. Significantly better agreement between the two data sets (a reduced χ^2 for a first-order Fourier fit to the combined sets of 2.0 versus 5.2) is achieved for a period of $3^{\rm d}_{\cdot}61860 \pm 0^{\rm d}_{\cdot}00017$. Adelman (1999, priv. comm.) communicates that this period is consistent with the Strömgren b-band photometric variation.

All magnetic measurements have therefore been phased according to the new ephemeris:

$$\mathrm{JD} = 2450001.881 + 3^{\rm d}_{\cdot}61860 \cdot \mathrm{E}, \qquad (12)$$

and are reported in Table 2. The epoch corresponds to a relatively recent date of longitudinal field maximum.

The phased LSD B_ℓ data are shown in Fig. 12 along with the measurements by Borra & Landstreet (1980). The two data sets are in good agreement. A least-squares first-order Fourier fit to the LSD measurements yields a reduced χ^2 of 3.6. As can be seen in Fig. 9 (dashed curve), this fit in particular matches very poorly the measurements near magnetic maximum. A second-order fit (solid curve) results in a much improved χ^2 of 1.4, suggesting that the longitudinal field variation of θ Aur probably differs from a pure sinusoid. The error bars associated with the LSD measurements are somewhat less than twice better than those of Borra & Landstreet, with a median of 33 G and a minimum of 22 G (versus a median of 55 G and a minimum of 40 G in the case of Borra & Landstreet). The precision however is limited only by the short integrations used for this star. This is consistent with the fact that most individual lines in the spectrum of θ Aur show very noisy or undetectable Stokes V signatures. The variation is detected at the 21σ level. These results show the power of LSD longitudinal field measurements for broad-lined ($v \sin i \gtrsim 50$ km s^{-1}) stars.

3.11 ϵ UMa

ϵ UMa is a broad-lined A0p star with a very weak magnetic field. WDLS reported LSD Stokes V profiles of ϵ UMa at 8 rotational phases. We have obtained B_ℓ measurements from each Stokes V profile. The measurements have been phased according to the ephemeris of Provin (1953):

$$\mathrm{JD} = 2434131.124 + 5^{\rm d}_{\cdot}0887 \cdot \mathrm{E}, \qquad (13)$$

and are reported in Table 2.

ϵ UMa has the weakest magnetic field ever measured in an A or B type star. The phased LSD B_ℓ measurements, along with Balmer-line Zeeman analyser measurements reported previously by Bohlender & Landstreet (1990b) and spectropolarimetric measurements reported previously by Donati et al. (1990), are shown in Fig. 13. The solid curve is a least-squares Fourier fit to the LSD measurements, with a reduced χ^2 of 0.46. The 3 data sets are all in reasonable agreement. The median uncertainty of the LSD measurements is 18 G, with a minimum of 15 G. This can be compared to median and minimum values for the Balmer-line Zeeman analyser measurements of 45 G and 35 G respectively, and for the spectropolarimetric measurements of 25 G and 20 G respectively. Again, the precision is limited by the short integrations used for this star. Using the LSD measurements, the variation is detected at the 6σ level.

3.12 HD 81009

WDLS obtained a single Stokes V, Q and U observation of this slowly rotating star which exhibits very sharp, resolved magnetically-split spectral lines. The rotational phase has been computing according to the ephemeris of Adelman (1997):

$$\mathrm{JD} = 2444483.42 + 33^{\rm d}_{\cdot}984 \cdot \mathrm{E}, \qquad (14)$$

and the measurement is reported in Table 2.

Figure 13. Longitudinal magnetic field measurement B_ℓ of ϵ UMa obtained from LSD profiles [solid circles], Hβ measurements by Bohlender & Landstreet (1990b) [open squares], spectropolarimeteric measurements by Donati et al. (1990) [asterisks]. The solid curve is a least-squares first-order Fourier fit to the LSD measurements.

The longitudinal field at this phase is consistent with additional measurements obtained by Wade et al. (1999b) in the context of a detailed study of the magnetic fields, component characteristics and orbital properties of this long-period SB1.

3.13 HD 126515

HD 126515 (Preston's star) is a sharp-lined A2p star with a strong magnetic field. WDLS obtained a single Stokes V, Q and U observation of this slowly rotating star. We have computed B_ℓ from the Stokes V LSD profile, and report this value in Table 2. We computed the phase assuming the ephemeris of Mathys & Hubrig (1997):

$$\mathrm{JD} = 2437015.0 + 129\overset{\mathrm{d}}{.}95 \cdot \mathrm{E}. \tag{15}$$

The observation is in agreement with both the results of Mathys & Hubrig as well as unpublished Balmer-line Zeeman analyser measurements communicated by Hill (1998, priv. comm.).

3.14 HD 153882

HD 153882 is a fairly broad-lined A2p star with a moderately strong magnetic field. WDLS obtained a single Stokes V and Q observation of this star. We have computed B_ℓ from the Stokes V LSD profile, and report this value in Table 2. We computed the phase assuming the ephemeris of Mathys & Hubrig (1997):

$$\mathrm{JD} = 2432752.730 + 6\overset{\mathrm{d}}{.}00890 \cdot \mathrm{E}. \tag{16}$$

The observation is in agreement with the results of Mathys & Hubrig (1997).

4 SUMMARY, DISCUSSION AND CONCLUSIONS

We have presented in this paper a new and alternative method for measuring the mean longitudinal magnetic field and net linear polarisation of magnetic A and B type stars. This method employs the Least-Squares Deconvolution procedure (LSD), developed by Donati et al. (1997) and first applied to circular and linear polarisation spectra of Ap and Bp stars by WDLS. The main advantages of this technique are: exploitation of effectively all strong metal lines available in the spectrum (blended and unblended); the production of a mean circular (or linear) polarisation profile which can indicate the existence of a magnetic field even when the longitudinal (or transverse) field component is null; and the association of an error bar with each spectral pixel in the LSD profile, which can be used to compute accurate error bars for any longitudinal field and net linear polarisation measurements obtained therefrom.

We have applied this technique to 14 stars for which WDLS have reported circular and/or linear polarisation LSD profiles. We present 129 new measurements of the mean longitudinal magnetic field of these stars as well as 124 measurements of the net linear polarisation. The stars range in spectral type from F0p through B9p, and exhibit projected rotational velocities from $\lesssim 3$ km s^{-1} to about 55 km s^{-1}.

The longitudinal field as measured from LSD profiles is in very good agreement with previously published measurements. This indicates that the assumption that LSD profiles can be analysed as individual spectral lines using Eq. (1) is verified. In every case this technique yields longitudinal field measurements which are more precise (by factors which can be larger in some cases by more than an order of magnitude) than those currently available.

The longitudinal field variation of stars with moderately strong and very strong fields are often detected at around the 50σ level (compared with only a few σ for many stars currently). Such a high S/N allows one to better characterise the detailed shapes of longitudinal field variations and to thereby infer the structure of the surface field and abundance distributions. Departures from pure sinusoidal variations were detected in the longitudinal fields of 4 stars (53 Cam, α^2 CVn, HD 32633 and θ Aur), and perhaps in that of 49 Cam as well. High S/N is also necessary for accurately determining the rotational periods of these stars. We have determined an improved period for 1 star (θ Aur) and critically tested the accuracy of a number of others. We also show that meaningful B_ℓ measurements can be obtained using lines of any single chemical element having enough available spectral lines (Fe, Cr and Ti in particular), and the reduction in precision of such measurements (as compared to that of a multi-element analysis) is basically consistent with the reduced number of spectral lines employed.

Net linear polarisation measurements have also been obtained from LSD Stokes Q and U profiles published by WDLS. For 4 stars details of individual measurements were reported. In several cases we find that the reduced χ^2s of least-squares Fourier fits to the net polarisation measurements are quite high, and probably suggest that the associated error bars are somewhat underestimated. For 4 stars the measurements have been compared with broadband linear polarisation measurements reported by Leroy (1995a).

Table 2. Longitudinal magnetic field measurements of magnetic A and B stars measured from LSD Stokes V profiles.

JD - 2450000	Phase	$B_\ell \pm \sigma_B$ (G)
53 Cam (HD 65339)		
496.449	0.949	-1895 ± 65
497.315	0.057	1398 ± 78
499.376	0.313	3345 ± 86
501.358	0.560	-1842 ± 70
502.405	0.691	-4602 ± 83
503.369	0.811	-4446 ± 103
505.468	0.072	1798 ± 74
849.393	0.919	-2740 ± 71
851.532	0.186	3232 ± 78
853.537	0.435	2030 ± 82
α^2 CVn (HD 112413)		
498.489	0.034	-697 ± 54
499.511	0.221	-424 ± 60
500.422	0.387	564 ± 48
501.470	0.579	469 ± 58
502.519	0.770	-571 ± 67
503.474	0.945	-585 ± 72
505.581	0.331	271 ± 57
852.539	0.767	-541 ± 46
854.539	0.133	-623 ± 44
856.524	0.495	629 ± 41
857.657	0.703	-226 ± 55
858.537	0.864	-728 ± 43
860.586	0.238	-288 ± 58
861.584	0.421	612 ± 42
862.515	0.591	406 ± 54
864.576	0.968	-686 ± 49
1194.600	0.308	228 ± 70
1198.633	0.045	-630 ± 66
78 Vir (HD 118022)		
498.565	0.236	-439 ± 43
499.607	0.516	-931 ± 39
500.509	0.759	-627 ± 51
502.583	0.316	-641 ± 48
503.551	0.576	-920 ± 64
850.712	0.848	-458 ± 45
851.665	0.105	-150 ± 25
852.608	0.358	-750 ± 46
853.669	0.643	-888 ± 43
854.610	0.896	-292 ± 37
855.612	0.165	-246 ± 32
856.618	0.435	-879 ± 41
858.623	0.974	-148 ± 23
862.596	0.041	-128 ± 20
863.516	0.289	-592 ± 49
865.580	0.843	-413 ± 49
1202.647	0.404	-899 ± 33
1203.644	0.672	-863 ± 40

JD - 2450000	Phase	$B_\ell \pm \sigma_B$ (G)
β CrB (HD 137909)		
500.615	0.489	-565 ± 29
849.661	0.370	-400 ± 22
852.708	0.535	-548 ± 28
854.706	0.643	-261 ± 24
855.705	0.697	-79 ± 20
856.704	0.751	171 ± 18
858.690	0.858	567 ± 20
859.630	0.909	695 ± 21
860.649	0.964	762 ± 24
861.651	0.019	745 ± 22
862.660	0.073	662 ± 20
863.679	0.128	511 ± 18
864.670	0.182	321 ± 16
865.639	0.234	107 ± 18
1192.681	0.925	760 ± 28
1198.701	0.251	60 ± 21
1209.694	0.845	530 ± 25
49 Cam (HD 62140)		
505.359	0.339	-1224 ± 59
849.558	0.632	-778 ± 43
850.577	0.870	1251 ± 41
856.407	0.230	-56 ± 46
857.518	0.488	-1542 ± 39
858.443	0.704	1 ± 47
859.535	0.959	1453 ± 40
860.490	0.182	387 ± 60
1194.413	0.078	1160 ± 71
1197.516	0.802	868 ± 42
1198.513	0.034	1330 ± 37
1204.502	0.431	-1686 ± 58
1209.603	0.621	-793 ± 82
1210.691	0.875	1354 ± 79
HD 32633		
850.416	0.244	1689 ± 56
851.366	0.391	219 ± 72
852.375	0.548	-1388 ± 98
855.442	0.025	-2243 ± 134
860.435	0.802	-3751 ± 215
861.394	0.951	-3832 ± 129
862.364	0.102	-466 ± 118
1198.385	0.360	994 ± 136
1201.478	0.841	-4106 ± 176
1202.434	0.990	-3123 ± 162
1203.448	0.147	630 ± 170
1204.452	0.304	1513 ± 156
1210.397	0.228	1392 ± 192

JD - 2450000	Phase	$B_\ell \pm \sigma_B$ (G)
HD 71866		
859.440	0.284	-122 ± 63
863.402	0.867	1549 ± 68
864.429	0.018	2013 ± 68
865.464	0.170	1422 ± 61
1192.471	0.251	360 ± 105
1193.501	0.402	-1384 ± 71
1194.753	0.586	-1591 ± 86
1201.596	0.593	-1490 ± 115
1204.657	0.043	2135 ± 81
1210.602	0.917	2021 ± 102
θ Aur (HD 40132)		
496.374	0.653	261 ± 33
497.282	0.904	-163 ± 38
499.481	0.512	272 ± 26
500.304	0.739	154 ± 30
501.321	0.020	-254 ± 56
502.311	0.294	145 ± 27
864.357	0.345	275 ± 25
865.420	0.639	232 ± 22
1192.446	0.013	-171 ± 71
1202.462	0.780	163 ± 45
1203.476	0.061	-192 ± 56
ϵ UMa (HD 112185)		
861.529	0.756	76 ± 28
862.575	0.962	89 ± 15
863.490	0.142	74 ± 18
864.550	0.350	-22 ± 23
865.555	0.547	-13 ± 19
1192.585	0.813	70 ± 16
1202.735	0.808	81 ± 17
1210.717	0.376	-32 ± 21
HD 24712		
857.333	0.234	610 ± 43
1192.313	0.124	1043 ± 58
1193.418	0.213	653 ± 86
1197.359	0.529	172 ± 42
HD 98088		
1197.617	0.341	917 ± 28
1202.590	0.183	484 ± 71
1203.555	0.346	937 ± 33
HD 81009		
1193.613	0.452	2661 ± 107
HD 153882		
500.684	0.611	-976 ± 69
HD 126515		
498.664	0.760	-874 ± 68

The agreement for 78 Vir and β CrB is good, while the agreement for 49 Cam and HD 71866 is somewhat poorer, although satisfactory. Such small differences are not unexpected, given the fundamentally different methods employed and the fact that we have made no effort to adapt the spectral range employed for LSD measurements to match that employed for the broadband measurements of Leroy (1995a). This generally good agreement suggests that net linear polarisation measurements are only weakly sensitive to any strong systematic errors which could result from these kinds of variables, and should therefore furnish valuable constraints on magnetic field structure. In addition, we point out that this general agreement allows us to confirm what has previously only been supposed: that the observed broadband linear polarisation does result from saturated Zeeman linear polarisation within spectral lines.

We have taken advantage of our new net linear polarisation measurements of α^2 CVn (for which useful measurements have not previously been published) to constrain the geometry of its magnetic field. When considered along with the B_ℓ measurements of Borra & Landstreet (1977), the linear polarisation data obtained for α^2 CVn imply a rotational axis inclination $i = 118°$ and magnetic axis obliquity $\beta = 72°$, with uncertainties of about 5° for each angle. If we assume that the dipole is centred, we obtain a polar strength $B_{\rm d} = 4.5$ kG. These results are reasonably similar to the centred dipole model described by Borra & Landstreet (1977).

The reduced χ^2s of Fourier fits to the LSD longitudinal field variations are all very close to 1.0, while fits to the net polarisation variations tend to be significantly higher. We have performed a statistical analysis of all fit reduced χ^2s, for both the longitudinal field and net polarisation variations (e.g. those shown for 78 Vir in Fig. 1), as well as their associated diagnostic N measurements (e.g. those shown for 78 Vir in Fig. 2). The histograms of the reduced χ^2s of the variations obtained from the diagnostic N LSD profiles, shown in Fig. 14 (lower frames), are effectively identical, with means of 1.1 and 1.2 and standard deviations of 0.4. These values are perfectly consistent with the expected distribution of χ^2s, and imply that the LSD error bars accurately represent the true observational scatter (e.g. Press et al. 1992). This shows clearly that the uncertainties associated with LSD longitudinal field and net linear polarisation measurements are not underestimated. The histogram of the longitudinal field reduced χ^2s, shown in Fig. 14 (upper left frame), exhibits a mean of 0.9 and a standard deviation of 0.4, and is similar to the N distributions. The histogram of the net linear polarisation reduced χ^2s, shown in Fig. 14 (upper right frame), is however very different from the others. The mean of the distribution is 2.7 and the standard deviation is 2.4, and the histogram exhibits a long, weak tail toward large (~ 10) values of χ^2/ν. Because we know the error bars associated with these measurements are accurate (see above), this strange distribution must result from inappropriateness of the model (i.e. of the Fourier fits). In fact, some stars (e.g. β CrB in Fig. 3, α^2 CVn in Fig. 6) are observed to exhibit rapid changes in the net polarisation with phase which are not well described by low-order Fourier fits. The reality of these rapid changes, which do not appear to be detected in broadband photopolarimetry, is verified by examination of the original LSD linear polarisation profiles (Wade et al. 1999a).

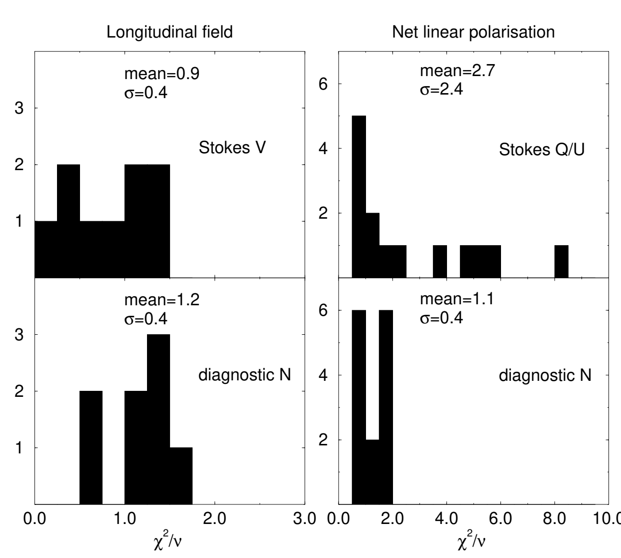

Figure 14. Distribution of reduced χ^2s of Fourier fits to LSD B_ℓ (at left) and net linear polarisation (at right) measurements. The upper frames show distributions from measurements of the V and Q/U mean signatures, while the lower frames show distributions from the measurements of the N mean signatures (c.f. Fig. 2). The Stokes V and N_V distributions are very similar, while the Stokes Q/U and $N_{Q/U}$ distributions differ significantly. Note the different vertical and horizontal scales.

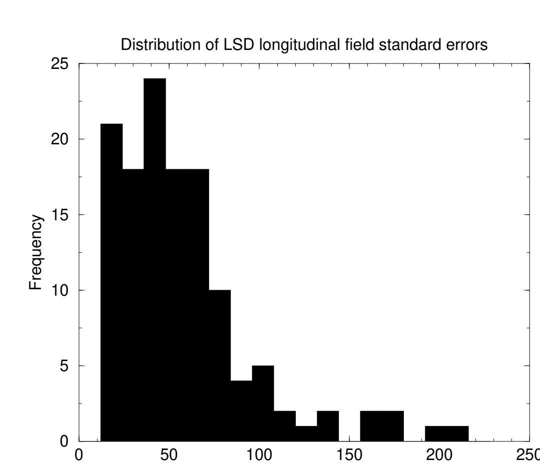

Figure 15. Distribution of standard errors associated with the longitudinal magnetic field measurements presented in this paper. Low precision outliers are almost all for faint ($m_V \sim 7$) stars.

The distribution of B_ℓ standard errors from this work is shown in Fig. 15. From this distribution we find the median multi-element B_ℓ uncertainty achieved in this study is 48 G, the mean B_ℓ uncertainty 58 G, and the standard deviation 38 G. The median likely provides the best estimate of the typical B_ℓ precision obtainable using this method as it is much more weakly influenced than the mean by rare extreme values of B_ℓ. 96% (114 out of 129) of the measurements presented in this paper have associated uncertainties smaller than 100 G, and most of those measurements with $\sigma_B > 100$ G are for faint stars ($m_V \sim 7$). This should be

Table 3. Net linear polarisation measurements of magnetic A and B stars obtained from LSD Stokes Q and U profiles. Each Q/U couplet is has been assigned a single JD and phase, computed from the midpoint of the combined observations.

JD - 2450000	Phase	$Q/I \pm \sigma_Q$ (%)	$U/I \pm \sigma_U$ (%)
	78 Vir (HD 118022)		
498.615	0.250	0.054 ± 0.007	-0.044 ± 0.006
499.657	0.529	-0.050 ± 0.007	0.009 ± 0.009
500.562	0.773	0.054 ± 0.008	-0.048 ± 0.006
503.597	0.588	-0.070 ± 0.017	-0.084 ± 0.017
850.741	0.856	0.072 ± 0.008	0.013 ± 0.007
851.701	0.114	-0.076 ± 0.006	-0.024 ± 0.007
852.659	0.372	0.029 ± 0.006	0.052 ± 0.007
853.714	0.655	0.000 ± 0.004	-0.075 ± 0.004
854.658	0.909	0.055 ± 0.004	0.053 ± 0.004
855.656	0.177	-0.028 ± 0.004	-0.054 ± 0.005
856.637	0.440	-0.025 ± 0.005	
858.654	0.982	-0.001 ± 0.006	0.064 ± 0.006
862.627	0.050	-0.044 ± 0.008	0.029 ± 0.008
863.562	0.301	0.060 ± 0.011	0.000 ± 0.010
865.610	0.851	0.074 ± 0.008	0.032 ± 0.012
1202.689	0.415	-0.011 ± 0.007	0.062 ± 0.007
1203.687	0.683	0.034 ± 0.006	-0.070 ± 0.007
	β CrB (HD 137909)		
500.645	0.491	0.026 ± 0.011	-0.001 ± 0.013
849.691	0.372	0.044 ± 0.008	0.044 ± 0.008
852.737	0.536	-0.008 ± 0.010	-0.017 ± 0.010
854.735	0.645	0.002 ± 0.008	-0.011 ± 0.008
855.736	0.699	0.000 ± 0.008	0.019 ± 0.008
856.733	0.753	0.002 ± 0.007	0.017 ± 0.008
858.717	0.860	0.076 ± 0.010	0.013 ± 0.010
859.659	0.911	0.084 ± 0.009	-0.051 ± 0.009
860.676	0.966	0.054 ± 0.012	-0.087 ± 0.011
861.680	0.020	-0.047 ± 0.009	-0.106 ± 0.009
862.687	0.075	-0.076 ± 0.010	-0.091 ± 0.008
863.706	0.130	-0.080 ± 0.010	-0.023 ± 0.009
864.702	0.184	-0.098 ± 0.009	0.039 ± 0.010
1192.717	0.927	0.130 ± 0.017	
1198.726	0.252	-0.041 ± 0.010	0.177 ± 0.010
1209.723	0.847	0.100 ± 0.016	0.042 ± 0.015

JD - 2450000	Phase	$Q/I \pm \sigma_Q$ (%)	$U/I \pm \sigma_U$ (%)
	α^2 CVn (HD 112413)		
498.521	0.040	-0.024 ± 0.081	0.025 ± 0.088
499.543	0.227	0.552 ± 0.056	-0.256 ± 0.056
500.456	0.393	-0.093 ± 0.059	0.102 ± 0.060
501.497	0.584	-0.301 ± 0.141	0.192 ± 0.169
502.549	0.776	0.237 ± 0.078	
503.507	0.951	-0.005 ± 0.190	-0.316 ± 0.174
505.705	0.353	-0.021 ± 0.086	-0.141 ± 0.088
852.573	0.773	0.290 ± 0.047	0.630 ± 0.048
854.572	0.139	0.092 ± 0.042	0.729 ± 0.047
856.556	0.501	-0.063 ± 0.044	-0.178 ± 0.042
857.685	0.708	0.098 ± 0.048	0.512 ± 0.049
858.565	0.869	0.362 ± 0.064	0.253 ± 0.060
860.616	0.244	0.620 ± 0.054	0.002 ± 0.052
861.616	0.426	-0.015 ± 0.051	-0.092 ± 0.055
862.544	0.596	-0.246 ± 0.070	0.162 ± 0.068
864.621	0.976	0.030 ± 0.120	0.048 ± 0.094
1194.621	0.312	0.224 ± 0.093	
1198.662	0.051	-0.124 ± 0.069	-0.034 ± 0.068
	49 Cam (HD 62140)		
505.417	0.353	-0.045 ± 0.025	-0.010 ± 0.023
849.603	0.642	0.057 ± 0.012	-0.037 ± 0.011
850.622	0.880	-0.003 ± 0.014	-0.041 ± 0.015
856.458	0.242	-0.001 ± 0.012	-0.012 ± 0.012
857.561	0.499	-0.066 ± 0.012	0.017 ± 0.012
858.486	0.715	0.042 ± 0.016	-0.025 ± 0.015
859.578	0.969	0.014 ± 0.016	0.000 ± 0.014
860.533	0.192	0.056 ± 0.026	0.002 ± 0.030
1194.705	0.146	0.060 ± 0.026	-0.008 ± 0.023
1197.564	0.813	0.040 ± 0.014	-0.066 ± 0.015
1198.559	0.045	0.061 ± 0.013	-0.029 ± 0.013
1204.545	0.441	-0.073 ± 0.019	0.057 ± 0.027
1209.645	0.631	0.098 ± 0.034	-0.027 ± 0.037

compared to the typical 1σ uncertainties of between 200 and 300 G obtained using other modern longitudinal field measurement techniques. The LSD technique improves upon this by a factor of between about 4 to 6. For individual stars the improvement is sometimes much better: in the case of 49 Cam our new LSD measurements improve on the typical standard error of measurements obtained using the Balmer-line Zeeman analyser technique by over an order of magnitude. This improvement, in our opinion, constitutes a redefinition of the standard of measurements of the longitudinal magnetic field.

The very small B_ℓ error bars achievable using LSD measurements, as well as the fact that LSD measurements produce a profile which can be potentially detected even in the case of zero longitudinal field, makes this technique particular suitable for searches for magnetic fields in weak-field Ap stars, as well as other types of stars in which weak or complex fields are suspected. For example, in the context of a search for magnetic fields in A, B and O type stars other than magnetic Ap stars (to be published separately; Shorlin et al. 1999) we have obtained LSD Stokes V profiles for some 30 Am, HgMn, λ Boo and Be stars with $v \sin i$ ranging from near zero to around 300 km s^{-1}. The median error bar for B_ℓ measurements obtained, for example, from profiles of the 19 Am stars is 17 G, over 3 times better than that obtained by the best previous studies, for a sample extending to considerably fainter objects.

The broad applicability of this technique to both faint and bright stars, with very small to quite large $v \sin i$, and throughout a wide range of spectral types makes it very useful for studying magnetic fields in all types of chemically peculiar stars, as well as for sensitive searches for magnetic fields in canonically nonmagnetic stars as well.

ACKNOWLEDGEMENTS

GAW acknowledges graduate scholarship support and post-doctoral support from the Natural Sciences and Engineering Research Council of Canada (NSERC), and research support from J.B. Lester and C.T. Bolton. JDL acknowledges grant support from NSERC. SLSS is supported under an Ontario Government Scholarship for Science and Technology. Our thanks to the referee S.J. Adelman for comments which contributed to the improvement of this manuscript.

REFERENCES

Abt H.A., Conti P.S., Deutsch A.J., Wallerstein G., 1968, ApJ 153, 177
Adelman S.J., 1997a, PASP 109, 9
Adelman S.J., 1997b, A&AS 122, 249
Babcock H.W., 1952, ApJ 116, 8
Babcock H.W., 1956, ApJ 124, 489
Bagnulo S., Landi Degl'Innocenti E., Landolfi M., Leroy J.-L., 1995, A&A 295, 459
Bohlender D.A. & Landstreet J.D., 1990a, MNRAS 247, 606
Bohlender D.A. & Landstreet J.D., 1990b, ApJ 358, 25
Bonsack W.K., 1976, ApJ 209, 160
Borra E.F. & Landstreet J.D., 1977, ApJ 212, 141
Borra E.F. & Landstreet J.D., 1980, ApJS 42, 421
Borra E.F., Landstreet J.D., Thompson I.B., 1983, ApJS 53, 151
Calamai G., Landi Degl'Innocenti E., Landi Degl'Innocenti M., 1975, A&A 45, 297
Catalano F.A. & Leone F., 1990, A&AS 83, 491
Catalano F.A. & Leone F., 1994, A&AS 108, 595
Donati J.-F., Semel M., Del Toro Iniesta J.C., 1990, A&A 233, 17
Donati J.F., Semel M., Carter B.D., Rees D.E., Cameron A.C., 1997, MNRAS 291, 658
Donati J.-F. & Wade G.A., 1999, A&A 341, 216
Donati J.-F., Catala C., Wade G.A., Gallou G., Delaigue G., Rabou P., 1999, A&AS 134, 149
Elkin V.G., 1998, in Proceedings of the 26th meeting and workshop of the European working group on CP stars, Cont. Ast. Obs. Skalnaté Pleso, p. 452
Farnsworth G., 1932, ApJ 76, 313
Glagolevski Yu.B. & Chutonov, 1998, in the proceedings of *Stellar Magnetic Fields*, Yu. V. Glagolevski & I.I. Romanyuk (eds.), Moscow
Hill G.M., Bohlender D.A., Landstreet J.D., Wade G.A, Manset M., Bastien P., 1998, MNRAS 297, 236
Kemp J.C. & Wolstencroft R.D., 1974, MNRAS 166, 1
Kurtz D.W., 1989, MNRAS 238, 261
Landstreet J.D., 1982, ApJ 258, 639
Landstreet J.D., 1988, ApJ 326, 967
Leroy J.-L., 1962, Ann. Astrophys. 25, 127
Leroy J.-L., 1995a, A&AS 114, 79
Leroy J.-L., 1995b, in *La polarimétrie outil pour l'étude de l'activité magnétique solaire et stellaire*, N. Mein and S. Salah-Bréchot eds., Observatoire de Paris, pp.
Leroy J.-L., Landolfi M., Landi Degl'Innocenti M., Landi Degl'Innocenti E., Bagnulo S., Laporte P., 1995, A&A 301, 797
Leroy J.-L., Landolfi M., Landi Degl'Innocenti E., 1996, A&A 311, 513
Mathys G., 1989, Fund. Cosmic Phys. 13, 143
Mathys G., 1991, A&AS 89, 121
Mathys G. & Hubrig S., 1997, A&AS 124, 475
Mathys G., Hubrig S., Landstreet J.D., Lanz T., Manfroid J., 1997, A&AS 123, 353
Preston G.W., 1969, ApJ 158, 243
Press W.H., Teukolsky S.A., Vetterling W.T., Flannery B.P., 1992, *Numerical Recipes in C, The Art of Scientific Computing, Second Edition*, Cambridge University Press, p. 661
Provin S.S., 1953, ApJ 118, 489
Pyper D.M., 1969, ApJS 18, 347
Renson P., 1984, A&A 139, 131
Ryabchikova T.A., Landstreet J.D., Gelbmann M.J, Bolgova G.T., Tsymbal V.V., Weiss W.W., 1997, A&A 327, 1137
Shore S.N. & Adelman S.J., 1976, Ap.J. 209, 816
Shorlin S.L.S., Wade G.A., Landstreet J.D., Donati J.-F., 1999, MNRAS, in preparation
Wade G.A., Elkin V.G., Landstreet J.D., Leroy J.-L., Mathys G., Romanyuk I.I., 1996, A&A 313, 209
Wade G.A., Elkin V.G., Landstreet J.D., Romanyuk I.I., 1997, MNRAS 292, 748
Wade G.A., Donati J.-F., Landstreet J.D., Shorlin S.L.S., 1999a, MNRAS, in press (WDLS)
Wade G.A., Debernardi Y., Bohlender D.A., Hill G.M., Landstreet J.D., Mathys G., Elkin V.G., 1999b, A&A, in preparation